

Adsorption behavior of poly(ethylene oxide) on kaolinite: Experimental and molecular simulation study

Tingting Wang¹, Jing Wang¹, Mingqing Zhang^{1,2}, Bingfeng Liu¹, Haijun Zhang², Jihui Li³

¹ School of Environmental Science & Spatial Informatics, China University of Mining & Technology, Xuzhou 221116, Jiangsu, China

² Chinese National Engineering Research Center of Coal Preparation and Purification, China University of Mining & Technology, Xuzhou 221116, Jiangsu, China

³ School of Chemical and Environmental Engineering, China University of Mining & Technology Beijing, Beijing 100083, China

Corresponding author: zmqcumt@163.com.cn (Mingqing Zhang)

Abstract: Poly(ethylene oxide) (PEO) adsorption behavior on kaolinite surfaces in an aqueous solution was investigated through experiments, the density functional theory (DFT), and molecular dynamics (MD) simulations. The experimental results showed that as the PEO concentration increased, the adsorption capacity first increased then slightly decreased and the turbidity change was opposite. The adsorption isotherm on the kaolinite surface was more suitable for the Langmuir model and valid for single-layer adsorption. The results of simulations showed that the PEO chains extended along the two basal surfaces of kaolinite or were partly adsorbed, forming loops and tails that caused most of the particles to flocculate, contributing to the turbidity lowering. When the number of PEO chains was excessive, their self- and inter-aggregation occurred with some PEO far from the surface, and the turbidity increased. On the kaolinite (001) surface, the hydrogen bonds between the PEO ether O and the hydroxyl groups constituted the main interaction mechanism. However, the hydrophobic force of the (CH₂-CH₂)-moiety of PEO might have dominated its adsorption on the (00 $\bar{1}$) surface. The hydrogen bonds were stronger than the hydrophobic interactions.

Keywords: kaolinite, poly(ethylene oxide), adsorption behavior, density functional theory, molecular dynamics

1. Introduction

It has been reported that the average total mineral matter in raw coal clays is 60%–80% (Xu et al., 2003). Clay minerals usually exist in colloidal sizes less than 2 μm in coal tailings. Due to isomorphic substitution, the clay particles are usually negatively charged. The fine granularity and strong electronegativity of the particles makes it easier for coal tailings to form a stable suspension, making treatment processes such as flocculation, sedimentation, and dewatering more difficult (Liu and Peng, 2014). Improving the clay mineral settlement is the key to the effective treatment of coal tailings.

Kaolinite is the most abundant clay mineral in coal tailings (Xu et al., 2003). The 001 crystal faces are the main cleavage planes, and their proportion is the largest of the total surface area of the kaolinite particles. When Kaolinite is disintegrated along the 001 face, two different basal-terminated surfaces, the aluminum hydroxyl surface (001) and siloxane surface (00 $\bar{1}$), appear simultaneously (Underwood et al., 2016). Therefore, these two surfaces were the general research targets of most previous studies (Bish, 1993). Kaolinite particles also have (010) and (110) edge surfaces generated by broken covalent bonds. Luo et al. contended that dodecylamine could be adsorbed by polar head groups (DDA⁺) on the (001) plane surface through electrostatic attraction, more easily than on the (00 $\bar{1}$) plane surface and that non-polar head groups faced the solution (Luo et al., 2022). However, as the same ionic surfactant, the adsorption of Octadecyl trimethyl ammonium chloride on a kaolinite surface was investigated by Chen et al., and the results showed that its optimal adsorption energies of -104.230 kJ/mol on (00 $\bar{1}$) face were < -100.192 kJ/mol adsorbed on (001) surface (Chen et al., 2019). More negative adsorption energies

indicate more favorable adsorption. The main electrostatic attraction was supplemented by weak hydrogen bonds between the methyl hydrogen atoms on the polar head and the surface oxygen atoms [6].

Poly(ethylene oxide) (PEO), a non-polar flocculant, is widely used to aggregate colloidal particles into fast-settling flocs (Swenson et al., 1998). Additionally, it has been reported that PEO can selectively adsorb on kaolinite surfaces in coal-kaolinite mixtures and enlarge the size of kaolinite particles, resulting in entrainment reduction and flotation improvement (Liu and Peng, 2014). Flocculation requires flocculant adsorption on the particle surface, followed by the attachment of more particles to the adsorbed polymer molecules. Although the flocculation rate of floc growth has been extensively studied, its adsorption behavior and mechanism have received less attention (Swenson et al., 1998; Mpfou et al., 2003; Ren et al., 2021). Mpfou et al. (2003) investigated the influence of adding PEO on the shear yield stress, settling rates, and consolidation behavior of kaolinite dispersions. Based on the results from these macro tests results, it was deduced that PEO adsorbed via strong hydrogen bonding between the ether oxygen (Lewis base) and OH groups (Bronsted acid) associated with kaolinite surface aluminol and silanol groups (Mpfou et al., 2003). However, this conclusion lacks a direct theoretical basis. The first-principles calculation method based on density functional theory (DFT) is an effective theoretical tool for analyzing the adsorption mechanism on mineral surfaces at the molecular and atomic levels. The classical molecular dynamics (MD) method can be used to study the statistical properties of real minerals, such as the concentration distribution, radial distribution function, and diffusion coefficient (Ren et al., 2021). Based on DFT calculations, Wang et al. found that the adsorption energy of PEO on the (001) surface is > that on the (00 $\bar{1}$) surface of Kaolinite (Wang et al., 2022). However, other interesting questions, such as the influence of PEO concentration on flocculation, have not been addressed using these theoretical tools.

Therefore, this study aimed to offer a detailed understanding of the microscopic interaction mechanism of PEO on two different basal surfaces of Kaolinite using DFT and MD, incorporating settlement tests and adsorption thermodynamics analyses. The effect of the PEO concentration on the adsorption behavior was tested and simulated. This will have a far-reaching influence on the further understanding of the flocculation and sedimentation of kaolinite dispersions and promote the combination of experimental and theoretical research in coal tailing treatment.

2. Experiments and simulation

2.1. Materials and methods

The Kaolinite used in the experiment was obtained from Huaibei Jinyuan Kaolinite Company (China), with a purity of 98%. The average particle size (d_{50}) of kaolinite particles was 2.74 μm . Reagent-grade PEO with an average molecular weight of 6.0×10^5 was purchased from Sinopharm Chemical Reagent Co., Ltd. (China). Fresh stock solutions of PEO were prepared daily at a concentration of 1.0 g/L. All the dispersions were prepared using Milli-Q water.

2.2. Adsorption and settlement experiments

Adsorption experiments were conducted in a constant temperature shaking bath at 20 ± 0.1 °C. Kaolinite suspensions were prepared by adding 1 g of kaolinite powder to conical flasks containing 100 mL Milli-Q water. After sufficient dispersion, the required amount of PEO solution was added to the conical flask, and the flask was shaken for 4 h to reach adsorption equilibrium, which was determined by pre-test. Small aliquots of the suspensions were withdrawn and centrifuged at 3000 rpm for 10 min. The supernatant was analyzed for the equilibrium PEO concentration using the tannic acid method [11]. The PEO adsorption capacities (q_e , mg/g) were calculated using Eq. (1).

$$q_e = \frac{(C_0 - C_e) \times V}{m} \quad (1)$$

where C_0 and C_e denote the initial (mg/L) and equilibrium (mg/L) concentrations of PEO at different initial concentrations, respectively; m (g) and V (L) denote the weight of the kaolinite powder and total volume of the solution, respectively.

Supernatant turbidity was used to evaluate the macro influence of PEO adsorption on the flocculation and settling behavior. After the equilibrium suspensions settled for 30 min, 20 mL of the

upper portion was withdrawn, and the turbidity was measured using a WGZ-2000 turbidimeter (Hahc, Zhengzhou North and South Baidu Instrument Factory, China). All adsorption tests were conducted at natural pH (6–9). Each test was repeated thrice, and the resulting data were determined as the average of the three measurements.

2.3. Adsorption thermodynamics

For thermodynamic analysis, adsorption experiments were carried out at 25 °C, 30 °C, and 40 °C, respectively. The PEO initial concentration was controlled at 20 mg/L. The thermodynamic parameters were calculated using the van 't Hoff equations (Eqs. (2–3)) (Stepanov, 2005):

$$\Delta G^\theta = -RT \ln K_0 \quad (2)$$

$$\ln K_0 = -\frac{\Delta H^\theta}{RT} + \frac{\Delta S^\theta}{R} \quad (3)$$

where ΔG^θ (J/mol) denotes the Gibb's free energy change, R denotes the universal gas constant (8.314 J/(mol·K)), T denotes the Kelvin temperature (K), and K_0 (q_e/C_e) denotes the adsorption partition coefficient. ΔH^θ and ΔS^θ denote the enthalpy change (J/mol) and entropy change (J/(mol·K)), respectively.

2.4. Density functional theory calculations

The adsorption energies and electron densities based on DFT were calculated on periodic models using the software package DMol³ (Local Density Functional Calculations on Molecules) (Delley, 1995). Exchange-correlation energy calculations were performed using the GGA-PBE function (Perdew-Burke-Ernzerh of generalized gradient approximation) (Perdew et al., 1996). The Perdew-Burke-Ernzerhof functional with the generalized gradient approximation was used to determine the exchange-correlation energy. DFT semi-core pseudopotentials were used to treat the core electrons. Electronic eigenstates were created using a basis set of Double Numerical plus d-functions with an orbital cut-off radius of 3.5 Å. The iterative subspace technique developed by Pulay was used to hasten SCF convergence with a subspace size of 6. Using the Tkatchenko-Scheffler method for DFT-D dispersion corrections enhanced the accuracy of the Van Der Waals interactions (Tkatchenko and Scheffler, 2009). A conductor-like Screening Model (COSMO) was used to describe the solvent environment on the two kaolinite surfaces (Klamt and Schuurmann, 2009).

The computations were based on the Kaolinite, water, and PEO parameters. Their molecular structures are shown in Fig. 1. The parameters of kaolinite primitive crystal cells include $a = 5.153\text{Å}$, $b = 8.941\text{Å}$, $c = 7.390\text{Å}$, $\alpha = 91.930^\circ$, $\beta = 105.050^\circ$, $\gamma = 89.800^\circ$ (Mathur and Moudgil, 1997). The Kaolinite (001) and (00 $\bar{1}$) surfaces were modeled using 2×2×1 supercells. In the molecular simulation process, dimethyl ether molecules, the monomer of PEO, were used to assess the interaction of PEO with the two kaolinite surfaces (Wang et al., 2022). To obtain the most stable adsorption configurations for PEO, the PEO monomer was first spread flat at four different initial sites on symmetric circular structure seen from top view, as shown in Fig. 2. The best adsorption site was determined using the adsorption energy (E_{ad}), which was calculated as follows:

$$E_{ad} = E_{PEO-Kaolinite} - (E_{PEO} + E_{Kaolinite}) \quad (4)$$

where $E_{PEO-Kaolinite}$ is the total energy of the kaolinite surface with the PEO monomer, E_{PEO} , and $E_{Kaolinite}$ are the energies of the PEO monomer and kaolinite slab, respectively. The greater the negative adsorption energy, the more stable the PEO monomer on the surface.

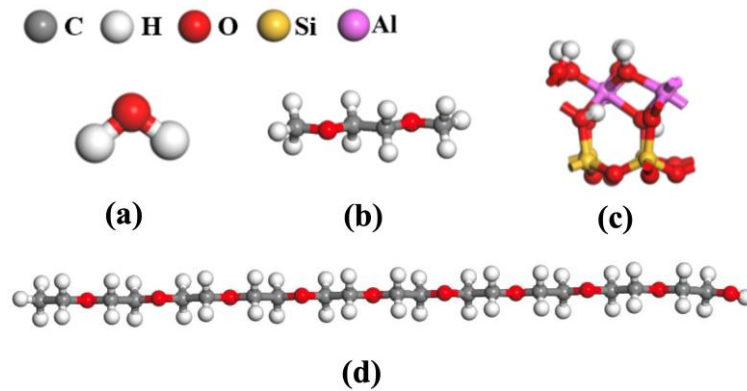


Fig. 1. Molecular structure of (a) water, (b) PEO monomer, (c) kaolinite unit cell, and (d) PEO chain

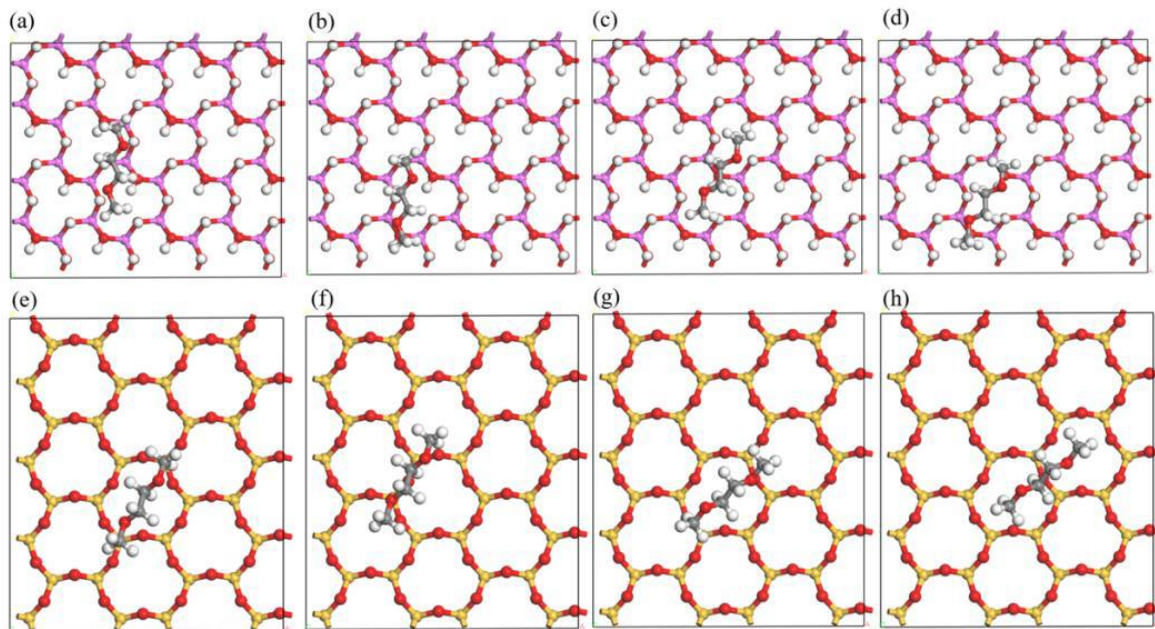


Fig. 2. The initial adsorption sites of PEO monomer on the surfaces of Kaolinite (001) (a-d) and Kaolinite (00 $\bar{1}$) (e-h)

2.5. Molecular dynamics simulations

MD simulations were performed using the Forcite module of the Material Studio software (version 8.0; Accelrys, San Diego, USA). First, the kaolinite cell was expanded to a $14 \times 9 \times 1$ supercell model and cleaved Kaolinite (001) and (00 $\bar{1}$) surfaces were used in these simulations. The PEO chains were built and packed into rectangular cells using an Amorphous Cell module. Annealing was then performed to eliminate the metastable PEO configurations. In this process, the initial temperature of the cell was set to 300 K, increased to 420 K, and then lowered to 300 K in steps of 10 K. Next, approximately 4000 water molecules were added to fill the rectangular cell to obtain the PEO structure model in a water environment. The build-layer tool was used to add a PEO and water system to the geometrically optimized supercells of martensite (001) and (00 $\bar{1}$) to construct a PEO, water, and kaolinite simulation system. Above the simulation system, a vacuum slab with a thickness of 80 Å was included to eliminate interaction between the adjacent slabs. The simulated system is shown in Fig. 3(a) and Fig. 3(b). Relevant information on the PEO is presented in Table 1.

In these simulations, a smart algorithm was applied to optimize the entire simulation system and minimize its energy consumption. A constant-volume and -temperature ensemble with a Nose thermost-

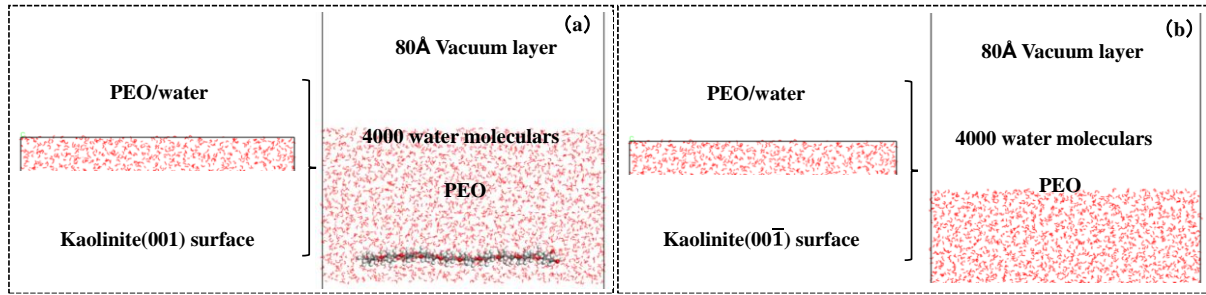


Fig. 3. The simulated systems of PEO adsorption on kaolinite/water interface, (a) Kaolinite (001) and (b) Kaolinite (00 $\bar{1}$)

Table 1 PEO information concerning the simulated systems

PEO name	Molecular number	Placement
PEO ₁	1×9-mer	1×1×1 array
PEO ₂	2×9-mer	2×1×1 array
PEO ₃	3×9-mer	3×1×1 array
PEO ₆	6×9-mer	6×1×1 array

Simulation was used in the three-dimensional periodic boundary condition. The conjugate gradient method was used to optimize the entire simulation system and reduce the residual force of each atom. Furthermore, a 1000 ps pre-equilibrium simulation was run with a time step of 1 fs. The last 500 ps output calculation was performed for the dynamic analysis.

3. Results and discussion

3.1. Adsorption and settlement test analysis

Flocculants with larger adsorption capacities were more conducive to capturing finer particles in the suspension. In this case, there were few residual particles in the supernatant, and the turbidity was correspondingly lower. The effects of the initial concentrations of PEO on the adsorption capacity of kaolinite and the turbidity of the supernatant are illustrated in Fig. 4. It can be seen that the adsorption capacity increased with the initial concentration increased until it reached the maximum value of 1.95 mg/g at PEO concentration 16 mg/L. Upon further increasing the PEO concentration, the adsorption capacity decreased slightly.

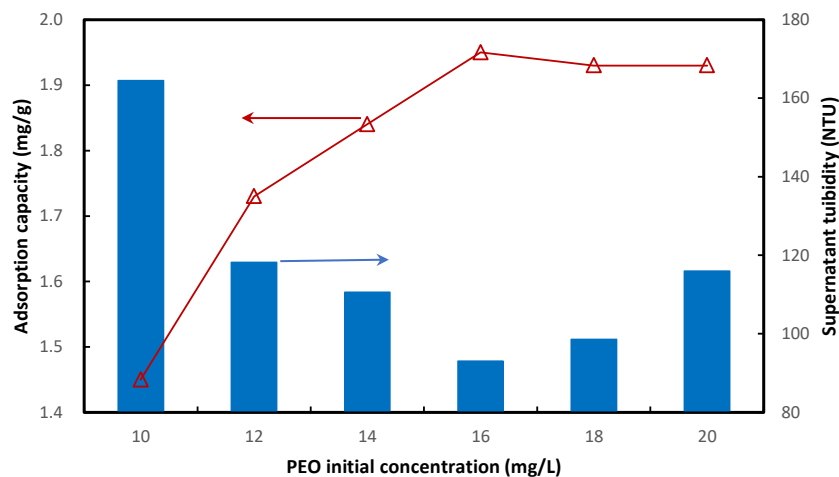


Fig. 4. Effect of PEO initial concentration on adsorption capacity and supernatant turbidity

However, the turbidity of the supernatant first decreased significantly and then increased with increasing PEO concentration. At 16 mg/L of PEO, the lowest turbidity reached a minimum of 93 NTU. The trend of turbidity change was consistent with the results of kaolinite suspensions flocculated by

other flocculants (Behl and Moudgil, 1993). This means that an excessive PEO dosage may inhibit the ability of the adsorbed PEO to capture more particles.

3.2. Adsorption thermodynamics analysis

Figure 5 shows the adsorption isotherms of PEO for Kaolinite at natural pH. These isotherms exhibit a strong affinity, with a steep increase in q_e at a significantly low equilibrium concentration C_e . Plateau coverage was achieved with $q_e = 1.71$ mg/g. The Langmuir and Freundlich models were used to fit the adsorption isotherms; the parameters are listed in Table 2. The correlation parameter (R^2) of the Langmuir adsorption model was closer to one than that of the Freundlich adsorption model. Therefore, the adsorption process was deemed more suitable for the Langmuir model. This indicates that the PEO might form a complete single-layer cover on the clay surface.

Table 2. Fitting parameters of Freundlich and Langmuir isothermal models for PEO on Kaolinite

Freundlich adsorption model		Langmuir adsorption model	
Parameters	Kaolinite	Parameters	Kaolinite
K_F (mg/g)	1.08	q_m (mg/g)	1.71
n	0.21	K_L (L/mg)	0.17
R^2	0.78	R^2	0.91

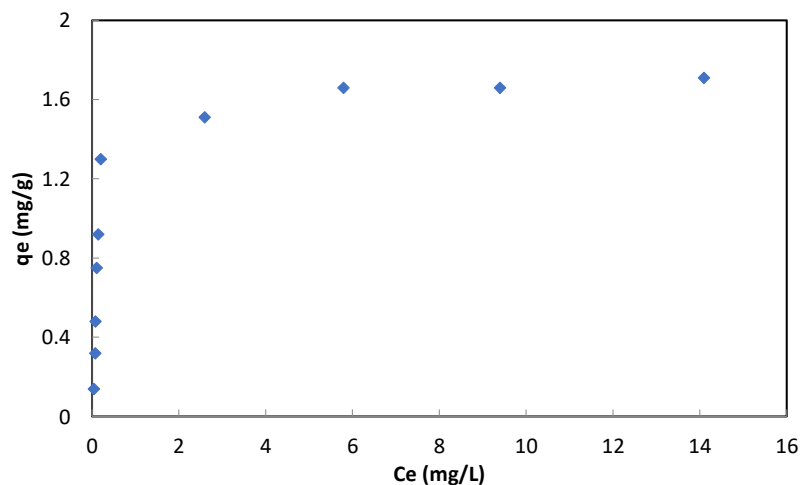


Fig. 5. Adsorption isotherms for PEO on kaolinite (temperature = 293 K)

The thermodynamic parameters of the adsorption process were calculated using Eqs. (2) and (3), and are listed in Table 3. All temperatures had negative ΔG^0 values for Kaolinite, and these values were of a magnitude comparable to the free energy of formation for 1 mol of hydrogen bonds (-20.9 kJ/mol). This suggests that hydrogen bonding significantly facilitates the spontaneous adsorption of PEO (Desiraju and Steiner, 2001). The positive ΔH values indicated that the adsorption process was endothermic, and the positive ΔS meant that the randomness of the interface increased with temperature during the adsorption process. The adsorption and desorption of water and PEO molecules occurred simultaneously on the kaolinite surface. The positive ΔS may result from the adsorption of PEO molecules and the desorption of a larger number of water molecules. The PEO molecules have a larger spatial volume than the water molecules.

Table 3. Thermodynamic parameters of PEO adsorption onto the surfaces of Kaolinite

Thermodynamic parameters	Temperature	Kaolinite
K_0 (dm ⁻³ mg ⁻¹)	298	188.09
	303	201.51
	313	238.61
ΔG^0 (KJ/mol)	298	-46.58

	303	-13.37
	313	-14.23
ΔH^{θ} (kJ/mol)	298	19.69
ΔS^{θ} (kJ/(mol.K))	298	0.11

3.3. Adsorption energies and electron density of PEO on kaolinite surfaces

Table 4 shows the adsorption energies of a single PEO monomer at different initial absorption sites on the Kaolinite (001) and (00 $\bar{1}$) surfaces. The adsorption energies on the Kaolinite (001) surface (-112.88 to -91.28 kJ/mol) are more negative than on kaolinite (00 $\bar{1}$) (-87.15 to -75.80 kJ/mol), which implies that the adsorption of the PEO molecule on the kaolinite (001) surface is more stable than on kaolinite (00 $\bar{1}$) surface, namely that the PEO molecule preferentially adsorb on the kaolinite (001) surface.

Table 4 Calculated results of adsorption energies of PEO on different absorption sites of Kaolinite (001) and surfaces and hydrogen bond length on (001) surface.

As shown in Fig. 6(a-d), two hydrogen bonds were formed between the PEO ethers O and H on the Kaolinite (001) surface, regardless of the initial site of the PEO monomer. The most stable adsorption model of PEO was model (a), with an adsorption energy of -112.88 kJ/mol, corresponding to the optimal equilibrium configuration as Fig.6(a). The electron density and Mulliken charge populations of the model (a) were analyzed and are shown in Fig. 7(a). The blue area in this figure indicates electron accumulation, whereas the yellow area indicates electron depletion; the greater the area of accumulation and depletion, the stronger the interaction between the PEO molecule and the kaolinite surface. The electron density increases for O on the Kaolinite (001) surface and decreases for H on the PEO monomer.

Table 4. Calculated results of adsorption energies of PEO on different absorption sites of Kaolinite (001) and surfaces and hydrogen bond length on (001) surface

Kaolinite (001)	Models	Adsorption energy (kJ/mol)	Hydrogen bond length (Å)
	Model a	-112.88	1.907, 2.030
	Model b	-91.28	2.044
	Model c	-103.00	2.09, 2.300
	Model d	-108.26	1.818
Kaolinite (00 $\bar{1}$)	Models	Adsorption energy (kJ/mol)	
	Model e	-85.62	
	Model f	-75.80	
	Model g	-87.15	
	Model h	-85.26	

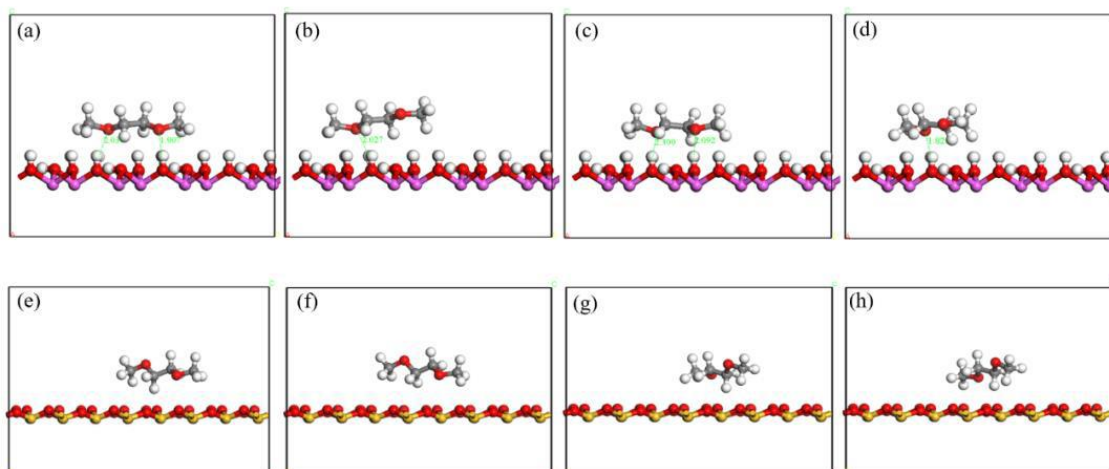


Fig. 6. The equilibrium configurations of PEO adsorbed on different initial absorption sites of kaolinite surfaces, (a-d) (001) and (e-h) (00 $\bar{1}$)

Similarly, the electron density decreased for H on the kaolinite (001) surface and increased for O on the PEO monomer. The total number of transferred electrons is approximately 0.518 eV. These results further confirmed the appearance of hydrogen bonds, which are the major contributors to the adsorption of PEO onto the Kaolinite (001) surface. Based on DRIFT spectral analysis, Behl *et al.* proposed that besides hydrogen bonding, hydrophobic interactions between the Si-O-Si surface and the ethylene group $-(CH_2-CH_2)-$ of the PEO monomer may also be an interaction mechanism; however, they are weaker than the hydrogen bonding mechanism (Xu *et al.*, 2003).

For the Kaolinite (00 $\bar{1}$) surface, Fig. 6(e)–(h) show no hydrogen bond formation. As shown in Fig. 7(b), the PEO molecule is opposite to the electron-accessible sites in the kaolinite 00-1 surface molecule, and the electron-losing sites in the PEO molecule are wrapped around the electron-accessible sites. Electrons are not transferred out of the kaolinite molecule. The small amount of charge transfer (0.03 eV) further illustrates this point. Therefore, the adsorption of PEO may have resulted mainly from hydrophobic interactions.

3.4. Structure and adsorption behavior of PEO on kaolinite surfaces

The first insight into microscopic structures can be gained by simply looking at snapshots obtained from MD simulations. Fig. 8 and Fig. 9 represent such snapshots of the increasing number of PEO chains on the Kaolinite (001) surfaces from the side and top views, respectively. At low concentrations of PEO (PEO₁), the PEO chains stretch out across the kaolinite surface, creating a loop-like structure. However, as the concentration of PEO increases to PEO₂, some atoms within the chain detach and form a tail-like structure. Upon increasing the amount of PEO to PEO₃ and PEO₆, self- and inter-aggregation occurred, and the carbon chain skeleton of PEO exhibited different degrees of distortion. Some molecular chains were located far from the surface rather than uniform adsorption. On the Kaolinite (00 $\bar{1}$) surface, the configurations of the PEO chains exhibited similar behaviors as the amount of PEO molecules increased, as shown in Fig. 10 and Fig. 11.

The spatial position and adsorption state of PEO on the kaolinite surfaces were also analyzed using the relative concentration profiles of PEO-O along the Z direction. The greater the cumulative number

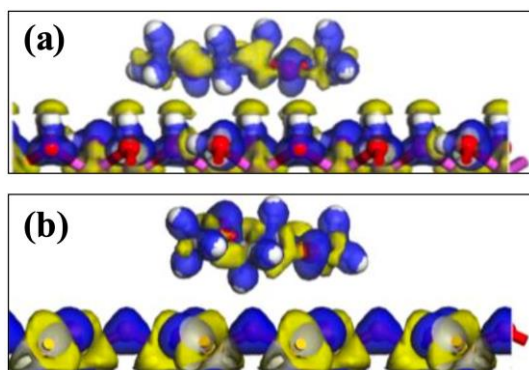


Fig. 7. Electron density difference for the most stable models of PEO monomer adsorbed on the surfaces of (a) kaolinite (001) and (b) (00 $\bar{1}$)

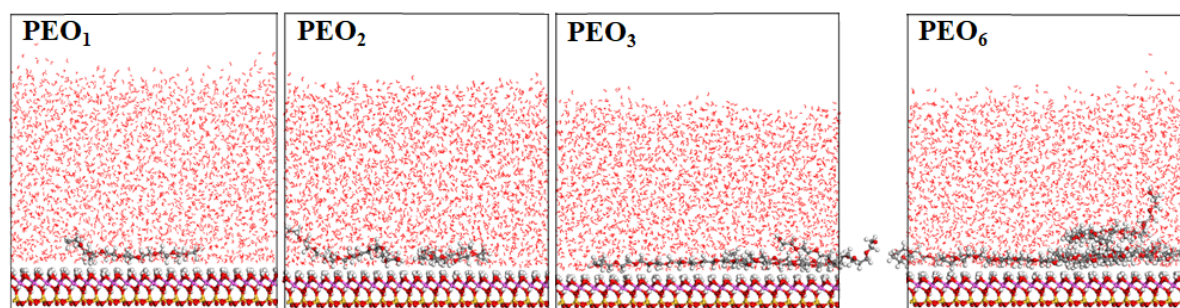


Fig. 8. The spatial equilibrium configurations of different numbers of PEO chains adsorbed on kaolinite (001) surfaces from side view

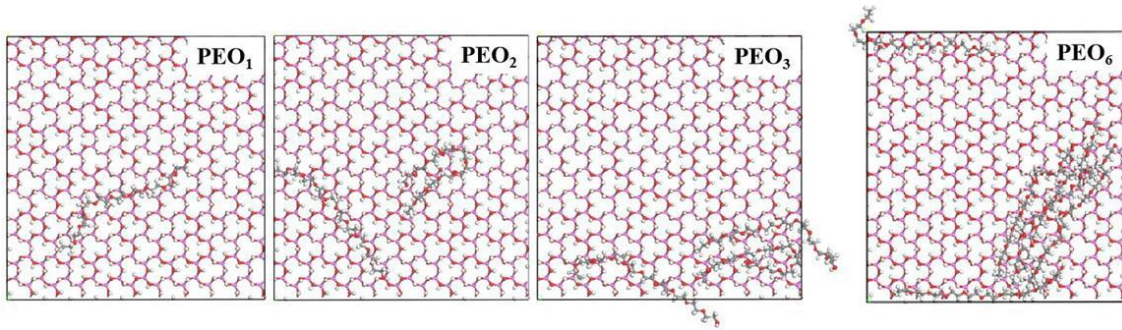


Fig. 9. The spatial equilibrium configurations of different numbers of PEO chains adsorbed on kaolinite (001) surfaces from top view

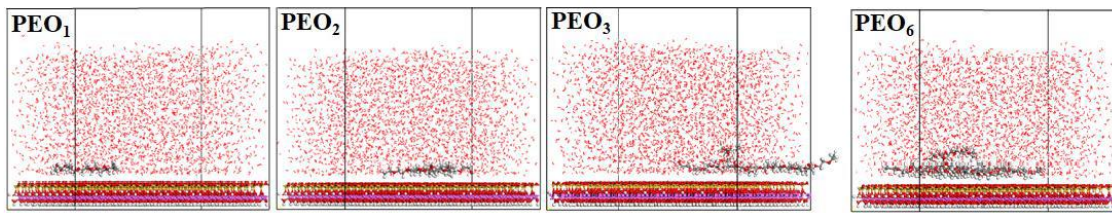


Fig. 10. The spatial equilibrium configurations of different numbers of PEO chains adsorbed on kaolinite (001) surfaces from side view

density of PEO-O, the more PEO adsorption on the surfaces. Fig. 12 (a) and (b) showed that with the number of PEO chains increased, the relative concentration of PEO-O first increased and then decreased, which corresponded to the phenomenon of some PEO chains far from the surface when excessive PEO appeared on the kaolinite surfaces shown in Fig. 8 and Fig. 10.

Considering that the water molecules and PEO may exhibit strong competitive adsorption on kaolinite surfaces, the true density distribution of H₂O-O on the two surfaces was calculated. The lower the number of water molecules, the higher the possibility of stronger PEO adsorption on the surface. Fig. 12(c) and Fig. 12(d) show that both base surfaces of Kaolinite exhibited a water layer structure in which water density reduction occurred in three stages. PEO appeared to decrease the water density. The density reduction on the Kaolinite (001) surface is more significant than that on the (001) surface, which may be related with the hydrophobic adsorption of PEO molecular. The order of H₂O-O density on the (001) surface was PEO₁ > PEO₂ > PEO₆ > PEO₃, which may result from some PEO chains being far from the (001) surface when PEO₆, as observed in the MD simulations.

Combined with the above analysis of the interaction energy, structure, and supernatant turbidity, we can safely conclude that hydrogen bonding plays a major role in the entire adsorption process compared to hydrophobic forces. When the PEO dosage was low, the polymer was preferentially adsorbed on the Kaolinite (001) surface via hydrogen bonds. Owing to the limited dosage of added PEO, capturing more particles to form flocs is difficult, resulting in higher supernatant turbidity. An increase

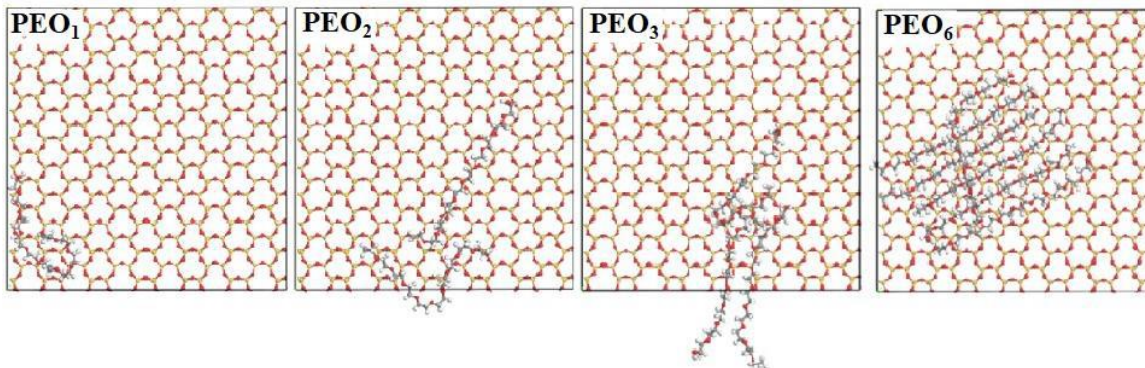


Fig. 11. The spatialequilibrium configurations of different numbers of PEO chains adsorbed on kaolinite (001) surfaces from side view

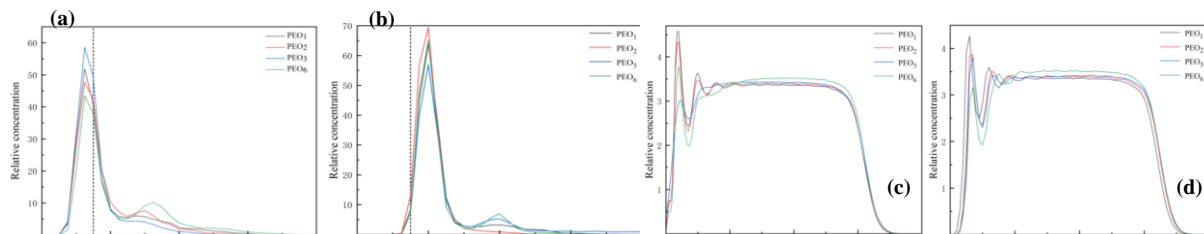


Fig. 12. The true density distribution of (a) PEO-O on kaolinite (001) surface, (b) PEO-O on kaolinite (00 $\bar{1}$) surface, H₂O-O on kaolinite surface (001) (c) and (d) H₂O-O on kaolinite surface (00 $\bar{1}$)

in PEO dosage can improve the probability and capacity of flocculant adsorption on kaolinite surfaces, and the turbidity of the supernatant gradually decreases. However, when the PEO molecular number is too high, the self- and inter-aggregation of PEO chains may hinder their stay close to kaolinite surfaces, and the turbidity rises.

4. Conclusions

The results of the settlement tests indicated that the turbidity of the supernatant first decreased and then increased slightly with increasing PEO concentration. The adsorption isotherm was deemed more suitable for the Langmuir model.

DFT calculations show that PEO is adsorbed mainly by forming hydrogen bonds between the PEO ether O and H on the Kaolinite (001) surface. However, the hydrophobic force from the $-(\text{CH}_2-\text{CH}_2)$ moiety of PEO may dominate its adsorption onto the (00 $\bar{1}$) surface. The adsorption energies of PEO monomer on different initial positions of the Kaolinite (001) surface are -112.88 to -91.28 kJ/mol, less than that on the Kaolinite (00 $\bar{1}$) surface with -87.15 to -75.80 kJ/mol, namely that PEO monomer more easily adsorbed on kaolinite (001) surface. The MD simulation results show that PEO chains extended along kaolinite surfaces or were partly adsorbed, forming loops and tails, and some self- and inter-aggregation appeared with increasing PEO chains, leading to some PEO far from the surface and an increase in supernatant turbidity.

Acknowledgments

This study was supported by the Natural Science Foundation of China (Grant No. 51874304 and No. 52004294).

References

- BEHL, S., MOUDGIL, B.M., 1993, *Mechanisms of Polyethylene Oxide Interaction with apatite*, J. Colloid Interface Sci. 161, 443-449.
- BISH, D., 1993, *Rietveld refinement of the kaolinite structure at 1.5 K*, Clays and Clay Minerals. 41(6) 738-744.
- CHEN J., MIN F., LIU L., LIU C., 2019, *Mechanism research on surface hydration of Kaolinite, insights from DFT and MD simulations*, Applied Surface Science 476(15), 6-15.
- DELLEY B., 1995, *DMol, a standard tool for density functional calculations: review and advances*, Theoretical and computational chemistry. 2, 221-254.
- DESIRAJU G.R., STEINER T., 2001, *The weak hydrogen bond. In Structural Chemistry and Biology*: Oxford University Press.
- KLAMT A., SCHÜÜRMAN G., 1993, *COSMO: a new approach to dielectric screening in solvents with explicit expressions for the screening energy and its gradient*, J. Chem. Soc. Perkin Trans. 2(5), 799-805.
- LIU D., PENG Y., 2014, *Reducing the entrainment of clay minerals in flotation using tap and saline water*, Powder Technology. 253, 216-222.
- LUO J., LIU M., XING Y., GUI X., LI J., 2022, *Investigating agglomeration of kaolinite particles in the presence of dodecylamine by force testing and molecular dynamics simulation*, Colloids and Surfaces A: Physicochemical and Engineering Aspects. 645, 128930.
- MATHUR, S. MOUDGIL B.M., 1997, *Adsorption mechanisms of polyethylene oxide on oxide surfaces*, Journal of Colloid and Interface Science. 196, 92-98.
- MPFOU P., ADDAI-MENSAH J., RALSTON J., 2003, *Investigation of the effect of polymer structure type on flocculation, rheology and dewatering behaviour of kaolinite dispersions*, Colloid Interface Sci. 71, 247-268.

- PERDEW J.P., BURKE K., ERNZERHOF M., 1996, *Generalized gradient approximation made simple*, Phys. Rev. Lett. 77 (18), 3865.
- REN B., LV K., MIN F., CHEN J., LIU C., 2021, *A new insight into the adsorption behavior of NPAM on kaolinite/water interface: Experimental and theoretical approach*, Fuel. 303(9), 121299.
- STEPANOV I.A., 2005, *The heats of chemical reactions: the Van't-hoff equation and calorimetry*, J. Zeitschrift für Physikalische Chemie. 219(8), 1089-1097.
- SWENSON J., SMALLEY M.V., HATHARASINGHE H.L.M., 1998, *Mechanism and strength of polymer bridging flocculation*, Physical Review Letters. 81(26), 5840.
- TKATCHENKO A., SCHEFFLER M., 2009, *Accurate molecular van der Waals interactions from ground-state electron density and free-atom reference data*, Phys. Rev. Lett. 102(7), 073005.
- UNDERWOOD T., ERASTOVA V., GREENWELL H.C., 2016, *Wetting effects and molecular adsorption at hydrated kaolinite clay mineral surface*, The Journal of Physical Chemistry C. 120(21), 11433-11439.
- WANG Y., CAO Y., HU S., 2022, *Effects of solution pH and polyethylene oxide concentrations on molybdenite–molybdenite, molybdenite–Kaolinite, and molybdenite–quartz interaction forces: AFM colloidal probe study*, Separation and Purification Technology. 380, 119926.
- XU Z., LIU J., CHOUNG J. W., ZHOU Z., 2003, *Electrokinetic study of clay interactions with coal in flotation*, International Journal of Mineral Processing. 68.1, 183-196.